

See discussions, stats, and author profiles for this publication at: <https://www.researchgate.net/publication/230830034>

Study on the interaction between gelatin and polyurethanes derived from fatty acids

ARTICLE *in* JOURNAL OF BIOMEDICAL MATERIALS RESEARCH PART A · APRIL 2013

Impact Factor: 3.37 · DOI: 10.1002/jbm.a.34407 · Source: PubMed

CITATIONS

4

READS

36

8 AUTHORS, INCLUDING:



[Gianluca Ciardelli](#)

Politecnico di Torino

155 PUBLICATIONS 2,393 CITATIONS

[SEE PROFILE](#)



[Virginia Cadiz](#)

Universitat Rovira i Virgili

169 PUBLICATIONS 2,975 CITATIONS

[SEE PROFILE](#)

Study on the interaction between gelatin and polyurethanes derived from fatty acids

R. J. González-Paz,¹ G. Lligadas,¹ J. C. Ronda,¹ M. Galià,¹ A. M. Ferreira,² F. Boccafroschi,³ G. Ciardelli,^{2,4} V. Cádiz¹

¹Department of Analytical and Organic Chemistry, Rovira i Virgili University, Tarragona 43007, Spain

²Department of Mechanical and Aerospace Engineering, Politecnico di Torino, Turin 10129, Italy

³Department of Clinical and Experimental Medicine, Università del Piemonte Orientale, Novara 28100, Italy

⁴CNR-IPCF UOS Pisa, Pisa 56124, Italy

Received 22 June 2012; revised 31 July 2012; accepted 2 August 2012

Published online 11 September 2012 in Wiley Online Library (wileyonlinelibrary.com). DOI: 10.1002/jbm.a.34407

Abstract: In this study, gelatin was blended to proprietary noncytotoxic polyurethanes (PU) derived from vegetable oils with different weight ratios, as material for the preparation of novel biomedical products. The PU/gelatin blends were characterized for their morphology through scanning electron microscopy. Mechanical and thermal properties, chemical interactions between components, degradation behavior, surface properties, cell adhesion, and bioactivity were investigated as a function of the protein content. Higher blend

miscibility was observed for the amorphous PUs, derived from oleic acid. Properties of PU/gelatin films were strongly influenced by the concentration of gelatin in the films. Gelatin enhanced the hydrophilicity, bioactivity, and cell adhesion of PUs. © 2012 Wiley Periodicals, Inc. *J Biomed Mater Res Part A* 101A: 1036–1046, 2013.

Key Words: polyurethane, fatty acid, gelatin, blend, bioactivity, immunocytochemistry

How to cite this article: González-Paz RJ, Lligadas G, Ronda JC, Galià M, Ferreira AM, Boccafroschi F, Ciardelli G, Cádiz V. 2013. Study on the interaction between gelatin and polyurethanes derived from fatty acids. *J Biomed Mater Res Part A* 2013;101A:1036–1046.

INTRODUCTION

Polyurethanes (PUs) are used in a wide variety of product applications in view of their extensive structure/property diversity such as excellent mechanical properties, elasticity and flexibility, high elongation, and good biocompatibility.^{1–5} During the past few decades, PUs have been widely used for biomedical applications such as vascular prostheses, catheters, and for skin and bone regeneration.⁶ In these applications, PU scaffolds demonstrated to support cell in-growth and tissue remodeling.^{7–15}

Vegetable oils are abundant biological materials and are used to obtain bio-based PUs because of their numerous advantages: low toxicity, inherent biodegradability, high purity, and noncytotoxic response. By modifying the chemical structure, these polymers will show different physical, chemical, and thermal properties and can become rigid or flexible, biostable or biodegradable, and cytocompatible or bioactive.^{16–21}

Blending has acquired importance in improving the performance of polymeric materials. It has become an economical and versatile way to obtain materials with a wide range of desirable properties. To ensure the homogeneity of the blends at microscopic level, resulting in superior material

properties, it is necessary to reduce the interfacial tension between the two constituent materials.²²

Blends of synthetic and natural polymers as proteins have been used in the last decades to develop new materials, the so-called “bioartificial polymeric materials.” Their capability of combining good physical and mechanical properties with biocompatibility characteristics was used with the purpose of making new materials for biomedical applications.^{23–27}

The combination of proteins with synthetic polymers should promote and stimulate enhanced cell and tissue compatibility of the synthetic matrix.²⁸ In general, all biological interactions (e.g., between cells, cells, and extracellular matrix) are mediated by specific biorecognition involving cell receptors which show high affinity to specific ligands. These ligands may be introduced into biomaterials by adsorption of extracellular matrix proteins on to a synthetic polymer. To engineer a cell–biomaterial interaction, it is necessary to understand the protein adsorption mechanism on a surface. The primary interaction between a protein and a substrate upon which it adsorbs is the hydrophobic effect. Hydrophobic surfaces tend to adsorb large amount of proteins with respect to hydrophilic ones. Secondary

Correspondence to: V. Cádiz; e-mail: virginia.cadiz@urv.cat

Contract grant sponsor: CICYT (Comisión Interministerial de Ciencia y Tecnología); contract grant number: MAT2011-24823

interactions involved in protein adsorption are electrostatic forces, resulting from opposite charges on a protein and the interacting surface.^{29,30}

Gelatin is a soluble extracellular matrix protein obtained by partial hydrolysis of collagen, the main fibrous protein constituent in bones, cartilages, and skin. This protein has chemotactic or adhesive properties: an Arg-Gly-Asp (RGD) amino acid sequence is found in the backbone of gelatin and serves as binding site for the cell receptors, thus improving cell adhesion, migration, and differentiation.^{31,32}

In this study, gelatin was blended to noncytotoxic PUs derived from vegetable oils²¹ with different weight ratios to develop novel bioartificial blends. Microscopic morphology, mechanical and thermal properties, chemical interaction, degradation tests, contact angle, cell adhesion, and bioactivity were investigated as a function of the protein content.

MATERIALS AND METHODS

Materials

Gelatin (bovine skin, type B) and hexafluoro-2-propanol (HFIP) were purchased from Sigma-Aldrich. PUs derived from fatty acids and 4,4'-methylenebis (phenyl isocyanate) (PUs) were synthesized as described in a previous study.²¹ All the analytical grade chemicals for preparing simulated body fluid (SBF) and used in the Western Blot analyses were purchased from Sigma Aldrich.

Preparation of SBF

SBF was prepared to create physiological fluid conditions according to Kokubo.³³ SBF was prepared by dissolving reagent grade chemicals (NaCl, NaHCO₃, KCl, K₂HPO₄·3H₂O, MgCl₂·6H₂O, CaCl₂, and Na₂SO₄ into distilled water). It was buffered to pH 7.25 with 50 mM Tris-HCl. SBF has a composition similar to human blood plasma.

Sample preparation

Gelatin was suspended in HFIP at room temperature under stirring overnight, PU was added, and the mixture was stirred at 40°C for 30 min until homogeneous solution was obtained. PU/gelatin films of various blending weight ratios (PU/gelatin = 100:0, 70:30, 90:10, and 0:100) were prepared by casting a 20 wt % blended solution in 10 mL of HFIP. The films were cast onto Petri dishes and then dried at room temperature for about 7 days until the solvent was completely evaporated. To eliminate any residual solvent, cast films were dried at 37°C for 48 h and stored in a vacuum desiccator.

Bioactivity evaluation and *in vitro* morphological changes

To study the bioactivity and morphological changes in SBF of PU/gelatin samples, films were cut into specimens of 5 × 20 mm² and immersed in 25 mL of SBF. The temperature was kept at 37°C in the shaking incubator (180 rpm) for up to 4 weeks and SBF solution was changed every 5 days. After being incubated for various periods of time (1–4 weeks), the specimens were removed from the SBF solutions, rinsed carefully several times with deionized water,

and subsequently dried for morphological analysis (scanning electron microscopy, SEM) and composition determination (energy-dispersive spectroscopy, EDS).

Morphological characterization (SEM-EDS)

The surface morphology and compositional changes were observed using a LEO 1430VP SEM-EDS Equipment. Prior to SEM-EDS examination, sample surfaces were coated with a conductive thin gold film.

Western blot antivinculin analyses for cell adhesion

NIH3T3 fibroblast cells were used. Fibroblast cells were cultured in Dulbecco's Modified Eagle Medium enriched with 10% fetal bovine serum, glutamine (2 mM), penicillin (100 U/mL), and streptomycin (100 µg/mL; Euroclone, Italy). Cells were maintained at 37°C in a humidified atmosphere with 5% CO₂ on the sample surfaces. Samples were seeded with NIH3T3 cells and cultured for 24 h. Culture medium was then discarded and a lysis solution (sodium dodecyl sulfate [SDS] 2.5%, Tris-HCl, pH 7.4, 0.25 M in bidistilled water) was placed on different samples. Cell proteins were quantified through BCA assay (Thermo Scientific). For electrophoresis, 10 µg of total proteins was used. Samples were diluted with Laemmli reducing buffer (60 mM Tris-Cl, pH 6.8, 2% SDS, 10% glycerol, 5% β-mercaptoethanol, 0.01% bromophenol blue), and electrophoresed on 7.5% SDS polyacrylamide gels (SDS-PAGE). The proteins were blotted onto nitrocellulose membranes. The membranes were incubated for 1 h in 5% blocking solution (nonfat dry milk in PBS), then incubated overnight with 1:500 dilution of primary antibodies (vinculin, Calbiochem, USA), followed by incubation with appropriate secondary antibody horseradish-peroxidase conjugate (Perkin-Elmer). Proteins were detected by Western Lightning plus-ECL (Perkin-Elmer), and protein bands were then visualized by Bio-Rad VersaDocTM imaging system (BioRad, Milano, Italy). Cells seeded on cell culture Petri dishes were used as positive control.

Beta-actin antibody (abcam, United Kingdom) has been used as loading control for Western blot analyses. In all, 10 µg of total proteins was used as performed for vinculin detection.

Contact angle

The hydrophilic/hydrophobic properties of the PU/gelatin-blended films were evaluated by contact angle measurements using CAM 200 KSV Instrument, equipped with Tetha software. Static contact angle measurements were carried out by addition of 5 µL drop of distilled water by a motor-driving syringe at room temperature on three different samples of each material and at least five measurements for each sample.

Mechanical tests

Stress-strain curves of PU/gelatin-blended films (10 × 5 × 0.1 mm³, length/width/thickness) were obtained at room temperature by means of a tensile testing machine MTS Qtest/10 Elite Controller, at a crosshead speed of 2 mm/

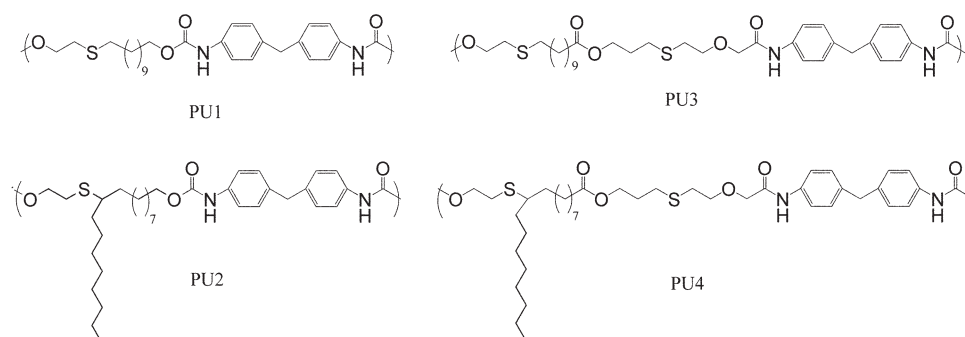


FIGURE 1. Chemical structures of PUs.

min. At least three specimens of each sample have been used.

Differential scanning calorimetry

Calorimetric studies were carried out on a TA DSC-Q20 instrument. Samples were accurately weighed (5.5 ± 0.5 mg) and sealed in hermetic aluminum pans. Dry nitrogen gas was purged into the DSC cell at a flow rate of 50 mL/min. DSC analysis was carried out at scanning rate of $10^\circ\text{C}/\text{min}$. An empty reference pan with the same weight was used as control.

Thermogravimetric analysis

Thermal stability studies of PU/gelatin-blended films were carried out on a thermogravimetric analysis (TGA) Q5 instrument (TA) with N_2 as a purge gas. The heating rate in TGA dynamic mode was $10^\circ\text{C}/\text{min}$ from 25 up to 600°C . Samples of 10 ± 0.5 mg were used.

Infrared spectroscopy by attenuated total reflection-Fourier transform infrared spectroscopy

Chemical characterization of PUs, gelatin, and PU/gelatin-blended films was performed by attenuated total reflection-Fourier transform infrared spectroscopy (ATR-FTIR), using a Frontier PerkinElmer FTIR spectrophotometer with universal ATR module (Diamond/KRS-5 crystal) in the $4000\text{--}400$ cm^{-1} wavenumber range. The spectra were analyzed by Spectrum 10TM software (PerkinElmer).

RESULTS AND DISCUSSION

The chemical structures of the previously synthesized oleic- and undecylenic acid-derived PUs (PU1–PU4) are shown in Figure 1. These PUs revealed good thermal and mechanical properties and no cytotoxic response,²¹ which make them promising materials for biomedical purposes. To prepare new bioartificial polymeric materials with good biocompatibility and high performance, blends of synthetic and natural polymers as gelatin were studied. Blends were prepared by mixing gelatin and PUs in HFIP obtaining a homogeneous solution, thus showing compatibility of the two components in HFIP solution. Blended films of PUs/gelatin were prepared by casting and the interaction of gelatin and PUs investigated.

Morphology of films

Figure 2 shows the SEM images of the blended films of PUs/gelatin with two blending weight ratios: 90:10 and 70:30, prepared by solution casting. The two micrograph images of PU1/gelatin [Fig. 2(a)] are the only ones showing clear indications of phase segregation of the two components. In all cases, observed fact is that as the blending concentration of gelatin increased, the roughness of the surface increased.

PU1 and PU3 derivatives from undecylenic acid showed higher crystallinity than PU2 and PU4 derivatives from oleic acid owing to the presence of long aliphatic pendant chains that hinder macromolecular chain packing. Thus, the higher flexibility of PU2 and PU4 chains benefits the miscibility of these PUs/gelatin blends as it appears in the higher homogeneity observed in the PU2/gelatin and PU4/gelatin micrographs.³⁴

Chemical and thermal properties

Chemical characterization of blended PUs/gelatin films was done by IR spectroscopy in the range of $1000\text{--}4000$ cm^{-1} by ATR-FTIR. As an example, Figure 3 shows the IR spectra of blended 90:10 and 70:30 PU1/gelatin films, together with PU3 and gelatin spectra. Characteristic absorption bands of main chain of PU3 were observed. $\text{C}=\text{O}$ stretching bands of urethane bonds appear at 1701 cm^{-1} , whereas the NH stretching and bending bands appear at 3323 and 1525 cm^{-1} respectively. Gelatin diagnostic absorptions, appear at approximately 1650 cm^{-1} (amide I) owing to stretching vibration of the $\text{C}=\text{O}$ bond, 3297 and 1540 cm^{-1} (amide II) corresponding to the NH stretching and bending bands, respectively, and 1280 cm^{-1} (amide III) corresponding to the stretching vibration of the $\text{C}-\text{N}$ bond. The presence of the amide III band is indicative of the triple helix structure of gelatin.³⁵ As it can be seen, the spectra of blended films showed common bands of PU1 and gelatin and notably an increase of the amide I and amide III bands is observed with increasing amount of gelatin in the blend.

The thermal degradation behavior of PUs, gelatin, and the blended samples was examined by TGA in nitrogen atmosphere. The thermal degradation of the different blends showed a similar behavior. As an example, the PU4/gelatin thermograms are collectively shown in Figure 4 together with those of PU4 and gelatin. Decomposition curves of

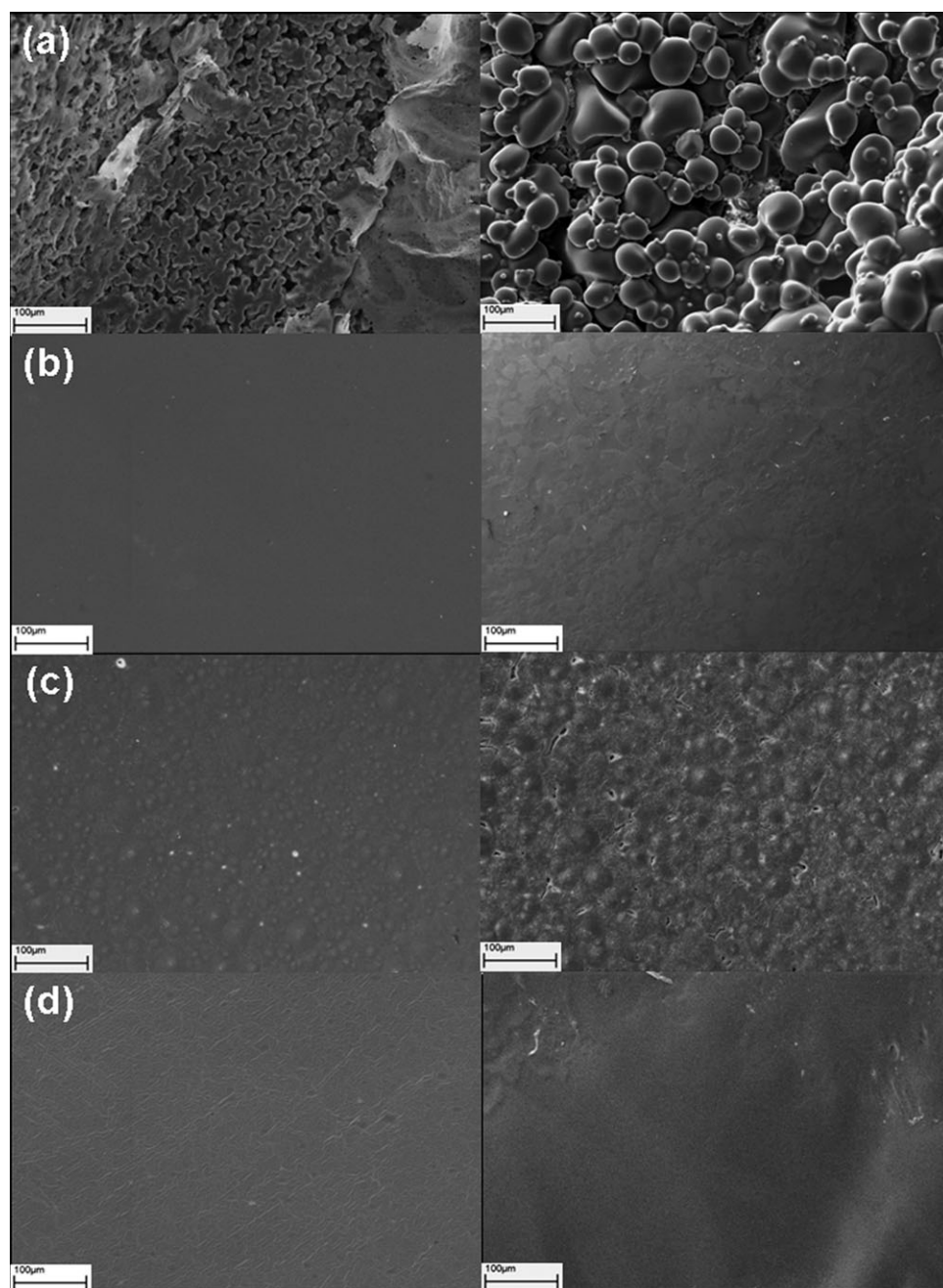


FIGURE 2. SEM images of 90:10 (left) and 70:30 (right) PU/gelatin-blended films. (a) PU1/gelatin, (b) PU2/gelatin, (c) PU3/gelatin, and (d) PU4/gelatin.

PU4/gelatin blends cast films show up to three overlapped degradation events. The first weight loss (8–10%) was attributed to dehydration of absorbed moisture and/or volatile components' evaporation. The second and third steps represent the sequence of pyrolytic reactions.²³

The thermal gravimetric curves show an event between 250 and 500°C which indicates the higher weight loss in all samples, which is characteristic of chemical degradation process, resulting from scission of urethane and peptide linkages in the polymer backbone. As shown in Figure 4, it is clear that the thermal stability regions of the blended

samples are at a temperature values comprised between those corresponding to the parent components and their stability decreases while increasing the gelatin content.

The effect on thermal transitions T_g and T_m arising from the different precursors was investigated by DSC (Table I). Figure 5 shows DSC traces for the different PUs/gelatin blends and their parent components. Gelatin (IV) presented a classical behavior: a glass transition ($T_g = 65^\circ\text{C}$) followed by helix coil transition or melting process ($T_m = 153^\circ\text{C}$). Gelatin is a denatured collagen and during the denaturation process, the triple helix structure of collagen is broken to

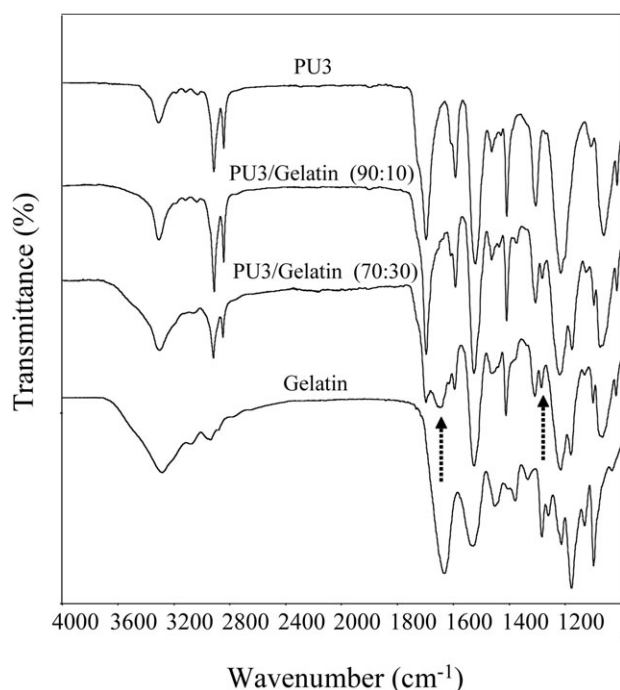


FIGURE 3. FTIR-ATR spectra of blended PU3/gelatin, PU3, and gelatin.

form random-coil gelatins. In an aqueous solution or specific organic solvents as HFIP,^{35,36} some gelatin chain can form secondary structures (helix) and three-dimensional network with zones of intermolecular microcrystalline junctions stabilized by the formation of interchain hydrogen bonds between C=O and N—H groups. In PUs, hydrogen bonding also exists between the same groups; consequently, it is now a well-known strategy to enhance the compatibility of PUs/gelatin blends by the incorporation of procedures described in Ref. ³⁴. The formation of intermolecular hydrogen bonds between PUs and gelatins not only promotes the miscibility of PUs/gelatin blends but also modifies the properties of the PUs.

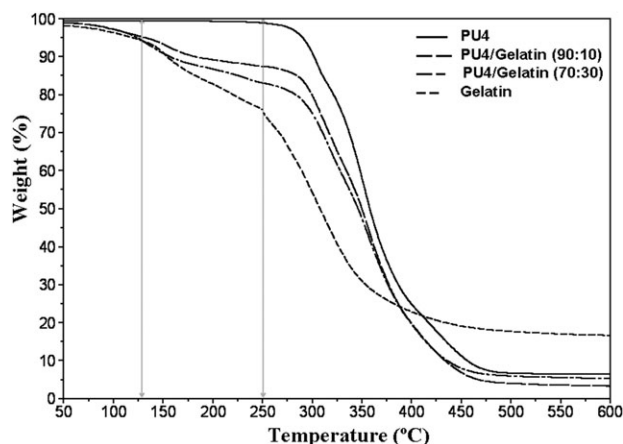


FIGURE 4. Thermograms of PU4, gelatin, and blended PU4/ gelatin.

The decrease of the melting point of a crystalline polymer component in a blend provides important information about its miscibility and its associated polymer–polymer interaction. In some blends, the hydrogen bonds are so strong that the crystallization of the crystalline components is hindered. Coherently, as shown in Figure 5, thermograms of blended PU3/gelatin (II and III) show that the melting point (T_m) and the enthalpy of melting (ΔH_m) of PU3 decreases with increasing gelatin content in the blends, and the crystallization of gelatin is suppressed in both cases. In contrast, the blended PU1/gelatin films (II and III) show only slight changes in T_m and ΔH_m compared to PU1 (I). Moreover, although the endotherm of melting process of gelatin is suppressed, its T_g remains at 63°C. These results are in accordance with the abovementioned phase segregation of the two components observed by SEM [Fig. 2(a)].

Literature concerning hydrogen-bonded polymer blends demonstrate that, in general, a positive or negative deviation from linearity of the blend T_g is observed,³⁴ and that is the case for the blends from amorphous PU2 and PU4 precursors. Moreover, as it can be observed in the thermograms of these blends, the melting process of gelatin is diminished or inhibited as mentioned above for PU1 and PU3.

Contact angle

Cells adhere and spread more effectively on surfaces with suitable hydrophilicity than on hydrophobic surfaces. Thus, surface wettability, that influences cell adhesion and proliferation, was measured by the water contact angle (Fig. 6). Contact angles of the pure PUs show the highest hydrophobicity, whereas the gelatin has a higher wettability. As the concentration of gelatin increases in the blends, water contact angles significantly decrease. These results prove that the addition of a hydrophilic natural polymer such as gelatin improves the hydrophilic properties of PUs/gelatin blends.

Mechanical properties

In general, the mechanical properties of gelatin materials are not matching the requirements of most biomedical applications. This limitation can be overcome by blending

TABLE I. Thermal Properties of PUs/Gelatin Blends and Parent Components

Samples	DSC		
	T_g (°C)	T_m (°C)	ΔH (J/g)
Gelatin	63	153	16
PU1	56	133	35
PU1/gelatin (90:10)	63	134	33
PU1/gelatin (70:30)	63	137	32
PU2	25	—	—
PU2/gelatin (90:10)	5	149	10
PU2/gelatin (70:30)	30	—	—
PU3	20	122	42
PU3/gelatin (90:10)	—	108	30
PU3/gelatin (70:30)	—	104	14
PU4	8	—	—
PU4/gelatin (90:10)	−4	154	2
PU4/gelatin (70:30)	0	149	6

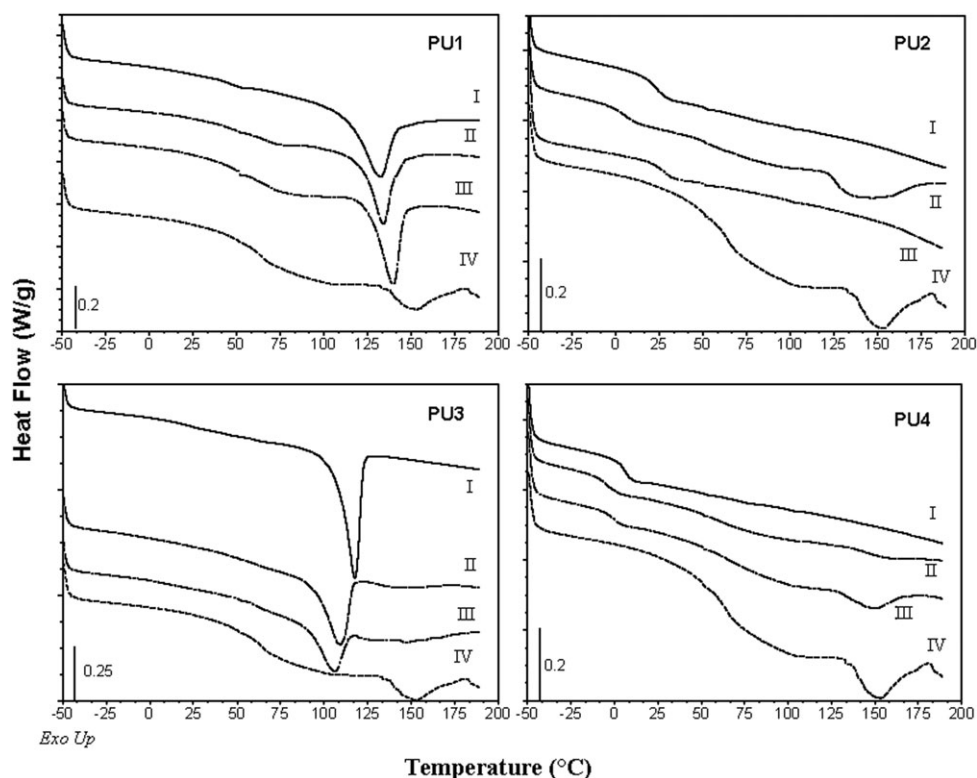


FIGURE 5. DSC traces of (I) PUs, (II) PUs/gelatin (90:10), (III) PUs/gelatin (70:30), and (IV) gelatin.

gelatin with other polymers of either natural or synthetic origin.^{23,32} In particular, for what concerns PUs, they exhibit much higher elasticity than most of the other polymers used in biomedical applications.⁶

The tensile stress-strain curves of blended PUs/gelatin films with different compositions are shown in Figure 7.

As it is evident in Figure 7, PUs/gelatin blends with composition of 10 wt % of gelatin (II) show a higher elongation at break in all samples, with the exception of PU1/gelatin blend. In this case, which presented phase segregation [Fig. 2(a)], both blended PUs/gelatin (II and III) showed lower mechanical properties than their pure compo-

nents (I and IV). Moreover, the combination of PUs and gelatin with a ratio of 30 wt % (III) increases the strength, but decreased the elongation at break of PU2 and PU3 blends. Only the combination of PU4 and gelatin with a ratio of 30 wt % (III) increases the mechanical properties, strength at yield, and elongation at break, and thus confirming appropriate interaction between PU4 and gelatin.³²

Morphology changes and bioactivity evaluation in SBF

Figure 8 shows morphological changes in PUs/gelatin blends as well as PU's control, during *in vitro* degradation after 1 week. With the exception of PU4/gelatin blend, in which the erosion rate is lower, it can be seen that the amount of gelatin dominates the morphology of the film. The higher the amount of gelatin loading the higher is the erosion on the surface, which is in agreement with the hydrophilicity of the blends, with consequently easier water diffusion.

A material is called "bioactive" when it has been designed to induce a specific biological activity.³⁷ The use of a bioactive material capable to nucleate calcium and phosphate ions on the surface of an implant may be advantageous, as bone formation can be accelerated as compared with the more inert metallic oxide surface of metallic implants. *In vivo* bioactivity can be predicted from *in vitro* tests using a SBF with a similar ion concentration to that of human blood plasma. In our experiments, the original SBF solution was used having the same composition proposed by Kokubo et al.³³ A material that rapidly forms bonelike calcium phosphates on its surface when immersed in SBF

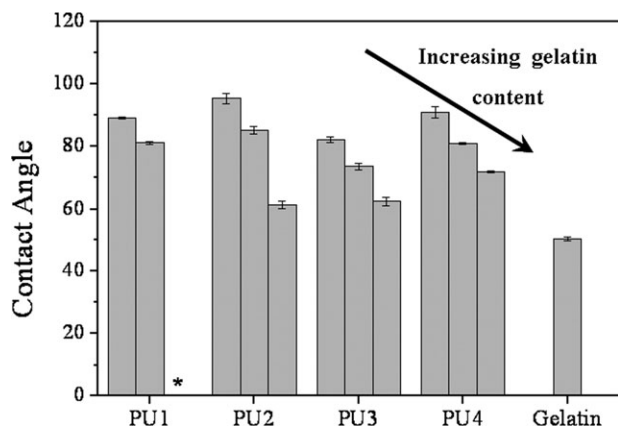


FIGURE 6. Contact angle values of PUs, gelatin, and blended PUs/gelatin. *Irregular sample surface to measure contact angle.

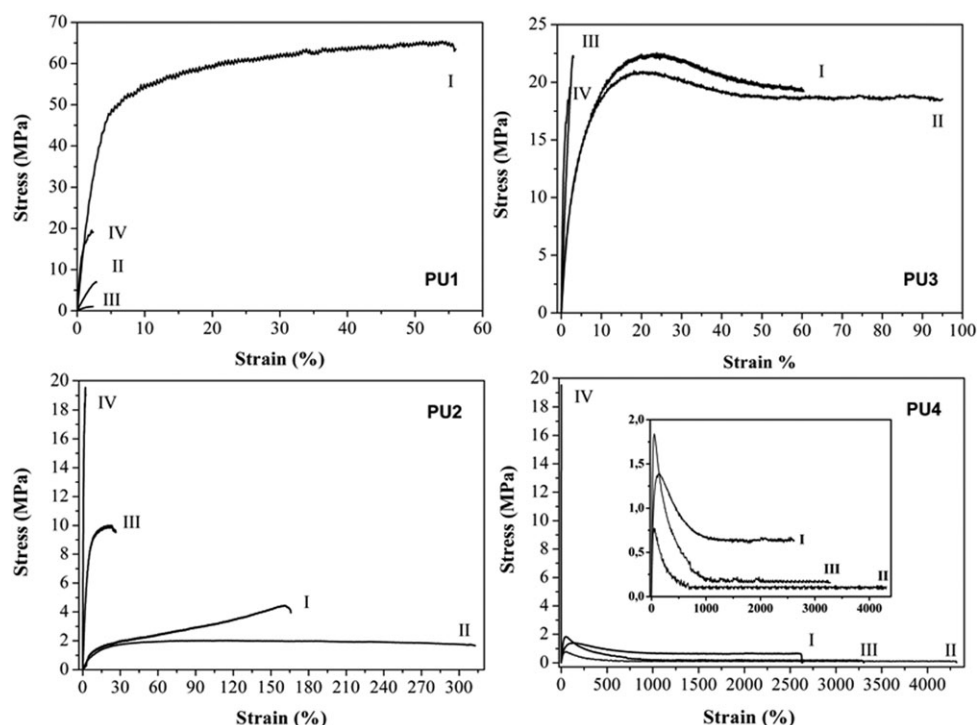


FIGURE 7. Stress-strain curves of (I) PUs, (II) PUs/gelatin (90:10), (III) PUs/gelatin (70:30), and (IV) gelatin.

will bond to living bone in a short period after implantation. This method can thus be used for screening the bioactivity of materials before *in vivo* animal testing. Recently, biomimetic deposition of calcium phosphate from SBF has been shown to be an effective method for coating many different types of polymers. In addition, the structure of biomimetic calcium phosphate may more closely match the structure of natural bone mineral and, therefore, enhance implant fixation and bone regeneration. The deposition of calcium phosphate crystals upon immersion in SBF has been generally attributed to ionic interactions between the scaffold surface and the SBF medium. In terms of being able to study calcium phosphates mineralization near-biological conditions, gelatin and oils have attracted some attention.³⁸ In Figure 9, the SEM micrographs of blended films of PUs/gelatin after bioactivity experiments are shown.

As it can be seen, after 2 weeks [Fig. 9 (a–d)], a significant difference is observed between the pure PUs and the PUs/gelatin blends. The first does not show mineral nucleation on the surface, whereas the blends do. However, this nucleation was observed on PU's surface after 4 weeks [Fig. 9(e–h)]. Composition EDS analyses on mineral content of all the samples are summarized in Table II.

The minerals on PU1/gelatin (90:10) and PU3/gelatin (70:30) blends' surface show the typical atomic composition of calcium phosphates contained in natural bone such as Mg, Na, or Cl, which can be introduced into the bone-like calcium phosphate lattice by substitution of one or more Ca atoms. However, the major substituent in biological bonelike calcium phosphates is carbonate which in bone mineral occurs, typically in 5–8 wt %.³⁹ PU1/gelatin (90:10) and PU3/gelatin (70:30) blends are the only ones that present

C-atoms in the compositional analyses by EDS after 2 weeks, and thus carbonate may be the mineral nucleated on surface. Other PUs/gelatin blends showed Ca/P ratios typical of biological calcium phosphates.⁴⁰ Thus, PU1/gelatin (70:30) has a Ca/P ratio of 2.15; this ratio is attributed to amorphous calcium phosphate (ACP), Posner⁴¹ proposed that ACP is the initially precipitating phase during bone formation *in vivo*. Ca/P ratio in PU2/gelatin (90:10) blend is 1, which is the Ca/P ratio found in pathological calcifications corresponding to dicalcium phosphate dihydrate (DCPD) and it is used in calcium phosphate cements for dentistry and other biomedical applications. PU2/gelatin (70:30) and PU3/gelatin (90:10) show Ca/P ratios very close to the value found for stoichiometric hydroxyapatite (1.67), which is a calcium phosphate similar to natural bone. Owing to chemical similarities to bone and teeth mineral, hydroxyapatite (HA) is widely used as coating for orthopedic and dental implants. PU4/gelatin blend shows a Ca/P ratio of 0.5, which corresponds to monocalcium phosphate monohydrate (MCPM) which is used in some calcium phosphate cements in medicine and mineral supplements for foods and beverages. Calcium phosphate nucleation was observed on pure PUs surface after 4-week SBF immersion; as summarized in Table II, they showed Ca/P ratios of 0.5 (MCPM) and 1 (DCPD). As conclusion, the bioactivity of the PUs is improved with gelatine and PU/gelatin blends showed mineral nucleation on the surface faster than the PUs.

Western blot antivinculin (131 kDa) analyses for cell adhesion

PUs derived from fatty acids used here to prepare the blends with gelatine, showed to be noncytotoxic.²¹

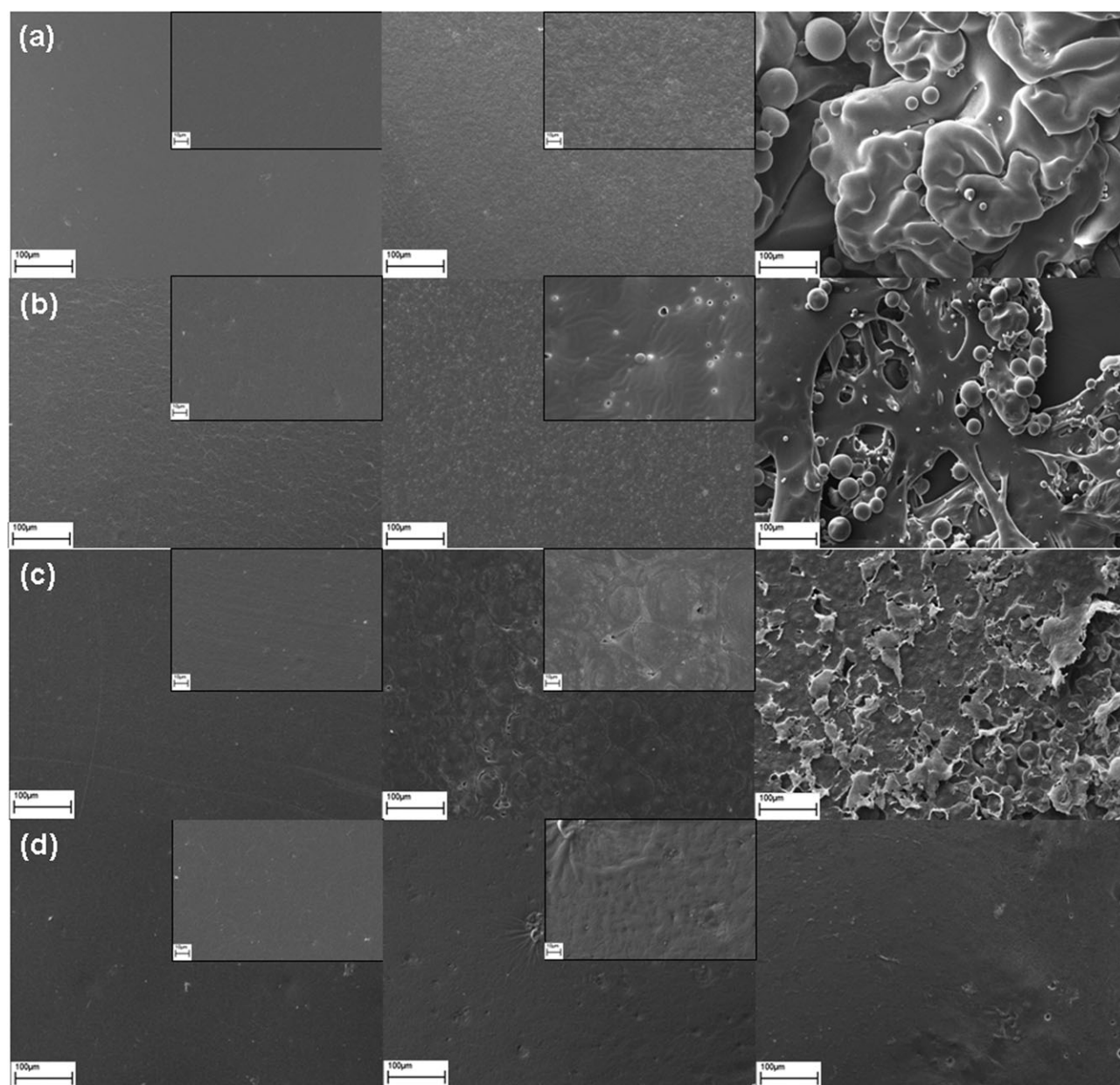


FIGURE 8. SEM images of degraded PUs (left) and PUs/gelatin blends 90:10 (middle) and PUs/gelatin blends 70:30 (right) in SBS solution, after 1 week. (a) PU1, (b) PU2, (c) PU3, and (d) PU4.

To further investigate the biocompatibility of these materials and to study the influence of the blended gelatine, cell adhesion assays were performed, by measuring vinculin expression through Western blot. Vinculin is a protein associated to focal adhesion of cells to substrates and adherent unions between cells and substrates. Focal adhesion quantification is a suitable method to measure biomaterial biocompatibility.⁴² For cytocompatibility testing, quantifying the amount of cell attachment should be proportional to the number of attached focal adhesion sites formed. Identifying a focal adhesion complex is possible by labeling any protein within it, using immunocytochemical cell adhesion identification (Western blot antivinculin analyses), which is a sensitive technique, as differences in adhesion to more subtly differ-

ing substrates could be detected by the difference in the protein expression. Increasing the expression of vinculin promotes cell adhesion and reduces cell motility.

In Figure 10, a higher vinculin expression is observed for amorphous PUs (PU2 and PU4) in comparison with semicrystalline PUs (PU1 and PU3). As expected, blending of PUs and gelatin improves cell attachment compared to pure PUs.

These results reflect the fact that cells require cell adhesion ligands (gelatin) for adhesion, but they also demonstrate that there might be an optimal ligand concentration and indicate that cell adhesion decrease, in most cases, in blends with a high concentration of gelatin. PUs/gelatin blends with composition of 10 wt % of gelatin have higher

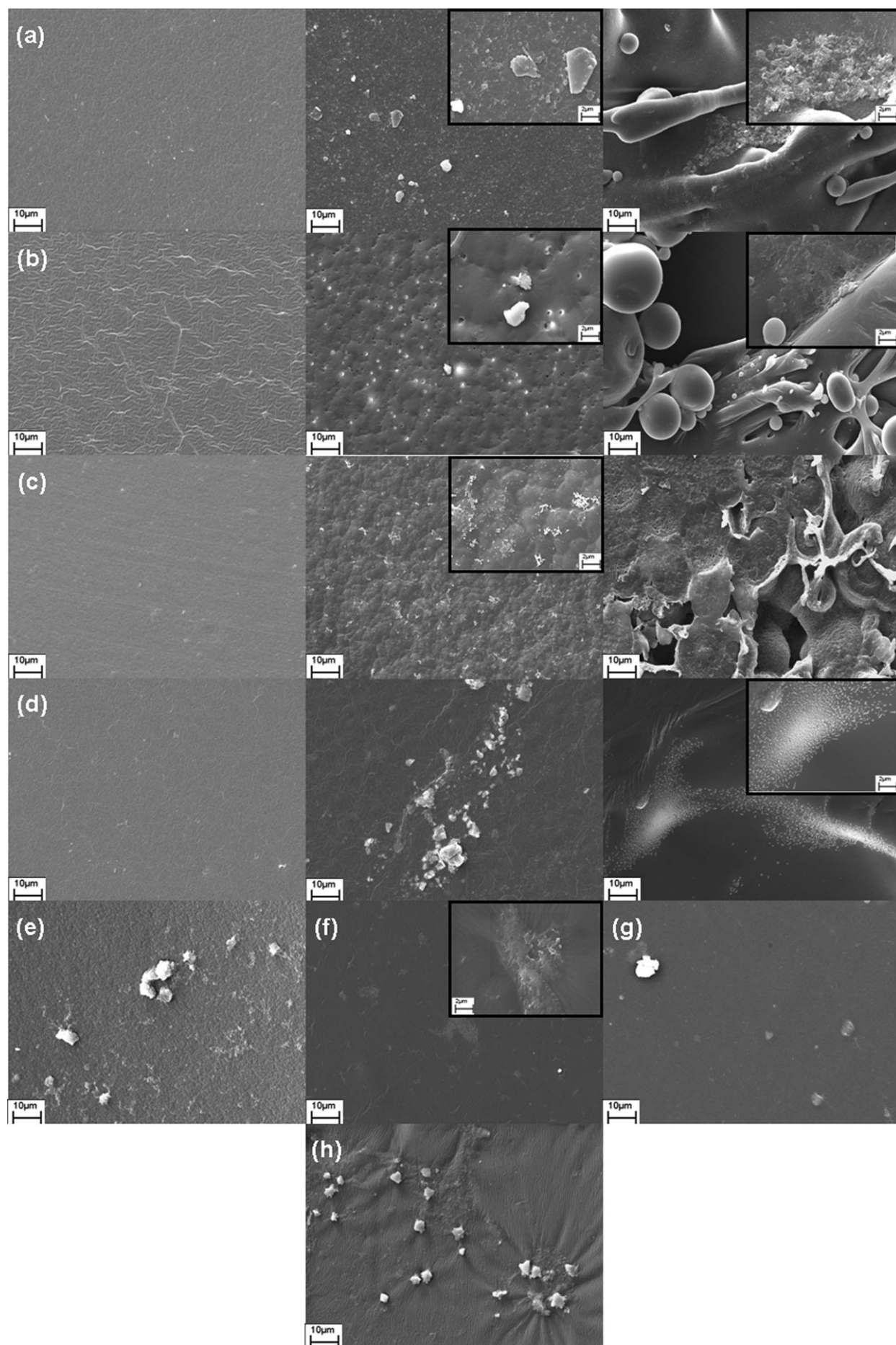


FIGURE 9. SEM images of PUs (left) and PUs/gelatin blends 90:10 (middle) and PUs/gelatin blends 70:30 (right) in SBS solution, after 2 weeks: (a) PU1, (b) PU2, (c) PU3, (d) PU4, and SEM images of pure PUs in SBF after 4 weeks: (e) PU1, (f) PU2, (g) PU3, and (h) PU4.

TABLE II. Composition Analyses on Mineral Content by EDS

Samples	Time (weeks)	Atomic (%)							Ca/P ratio
		Mg	C	Cl	Na	O	P	Ca	
PU1/gelatin (90:10)	2	16.9	34	–	–	47	–	1.8	–
PU1/gelatin (70:30)	2	–	–	–	–	89.42	3.35	7.23	2.15
PU2/gelatin (90:10)	2	–	–	–	–	97	1.5	1.5	1
PU2/gelatin (70:30)	2	–	–	–	–	94.38	2.11	3.51	1.66
PU3/gelatin (90:10)	2	–	–	–	–	94.89	1.9	3.21	1.68
PU3/gelatin (70:30)	2	–	71.06	0.98	0.78	24.35	–	2.83	–
PU4/gelatin (90:10)	2	–	–	–	–	90.17	6.52	3.31	0.50
PU4/gelatin (70:30)	2	–	–	–	–	97.78	1.47	0.75	0.51
PU1	4	–	–	–	–	–	1.88	0.89	0.47
PU2	4	–	–	–	–	97.37	1.78	0.85	0.48
PU3	4	–	–	–	–	98	1.01	0.99	0.98
PU4	4	–	–	–	–	74.99	11.91	13.1	1.09

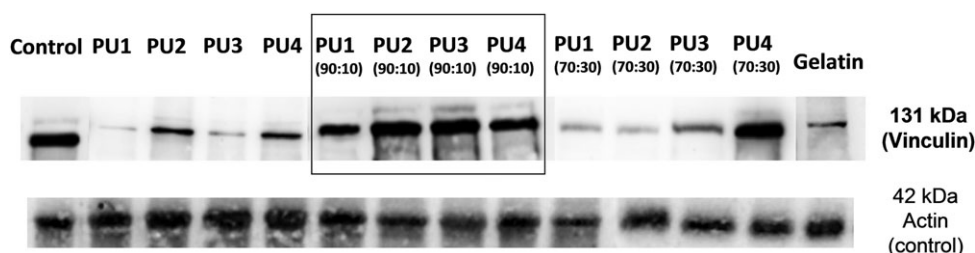


FIGURE 10. Western blot antivinculin (131 kDa) analyses on NIH3T3 fibroblast-like cells seeded on different substrates for 24 h.

expression of vinculin (comparable with positive control) than blends with composition of 30 wt % of gelatin. Only the combination of PU4 and gelatin with a ratio of 30 wt % presents a higher vinculin expression, comparable with control, in the blends. This could be attributed to the lower erosion rate presented on the surface of this blend [Fig. 8(d)]. Neff et al.⁴³ demonstrated that an intermediate RGD concentration on the surface provides maximum cell adhesion of fibroblasts, indicating that excessive peptide levels on the surface cause a decrease in cell adhesion.

CONCLUSIONS

In this study, gelatin was blended to proprietary noncytotoxic PUs derived from vegetable oils with different weight ratios. Higher blend miscibility was observed for the amorphous PUs, derived from oleic acid owing to the higher flexibility of their chains. Results demonstrate that the properties of PU/gelatin films were strongly influenced by the concentration of gelatine in the films. The hydrophilic gelatine improves the hydrophilic properties of the PU/gelatin blends with consequently easier water diffusion and a higher erosion on the surface. The bioactivity of the PUs is improved with gelatin, thus PU/gelatin films showed mineral nucleation on the surface faster than the PUs. Western blot analysis showed that adhesion ligands (gelatin) improved cell adhesion. Gelatin/PU films prepared would eventually be suitable for biomedical applications, such as orthopedic and dental implants.

ACKNOWLEDGMENTS

The authors express their thanks to CICYT (Comisión Interministerial de Ciencia y Tecnología) (MAT2011-24823) for financial support for this work.

REFERENCES

- Wirpsza Z. Polyurethanes: Chemistry, Technology and Applications. London: Ellis Norwood;1993.
- Król P. Synthesis methods, chemical structures and phase structures of linear polyurethanes. Properties and applications of linear polyurethanes in polyurethane elastomers, copolymers and ionomers. *Prog Mater Sci* 2007;52:915–1015.
- Chattopadhyay DK, Raju KVS. Structural engineering of polyurethane coatings for high performance applications. *Prog Polym Sci* 2007;32:352–418.
- Del Rio E, Lligadas G, Ronda JC, Galià M, Meier MAR, Cádiz V. Polyurethanes from polyols obtained by ADMET polymerization of a castor oil-based diene: Characterization and shape memory properties. *J Polym Sci Part A: Polym Chem* 2011;49:518–525.
- Vozzi G, Rechichi A, Dini F, Salvadori C, Vozzi F, Burchielli S, Carlucci F, Arispici M, Ciardelli G, Giusti P, Ahluwalia A. PAM-micro-fabricated polyurethane scaffolds: In vivo and in vitro preliminary studies. *Macromol Biosci* 2008;8:60–68.
- Vermette P, Griesser HJ, Laroche G, Guidoin R. Polyurethanes in Biomedical Applications. Texas: Landes Bioscience Press;2001.
- Silvestri A, Serafini PM, Sartori S, Ferrando P, Boccafroschi F, Milione S, Conzatti L, Ciardelli G. Polyurethane-based biomaterials for shape-adjustable cardiovascular devices. *J Appl Polym Sci* 2011;122:3661–3671.
- Zhang JY, Beckman EJ, Hu J, Yang GG, Agarwal S, Hollinger JO. Synthesis, biodegradability, and biocompatibility of lysine diisocyanate-glucose polymers. *Tissue Eng* 2002;8:771–785.
- Li B, Davidson J M, Guelcher SA. The effect of the local delivery of platelet-derived growth factor from reactive two-component

- polyurethane scaffolds on the healing in rat skin excisional wounds. *Biomaterials* 2009;30:3486–3494.
10. Hafeman AE, Li B, Yoshii T, Zienkiewicz K, Davidson JM, Guelcher SA. Injectable biodegradable polyurethane scaffolds with release of platelet-derived growth factor for tissue repair and regeneration. *Pharm Res* 2008; 25, 2387–2399.
 11. Guan J, Sacks MS, Beckman EJ, Wagner WR. Synthesis, characterization, and cytocompatibility of elastomeric, biodegradable poly(ester-urethane)ureas based on poly(caprolactone) and putrescine. *J Biomed Mater Res* 2002;61:493–503.
 12. Fujimoto KL, Guan J, Oshima H, Sakai T, Wagner WR. In vivo evaluation of a porous, elastic, biodegradable patch for reconstructive cardiac procedures. *Ann Thorac Surg* 2007;83:648–654.
 13. Gorna K, Gogolewski S. Preparation, degradation, and calcification of biodegradable polyurethane foams for bone graft substitutes. *J Biomed Mater Res A* 2003;67:813–827.
 14. Adhikari R, Gunatillake PA, Griffiths I, Tatai L, Wickramaratna M, Houshyar S, Moore T, Mayadunne RTM, Field J, McGee M, Carbone T. Biodegradable injectable polyurethanes: Synthesis and evaluation for orthopaedic applications. *Biomaterials* 2008;29:3762–3770.
 15. Zunfeng L, Xiang W, Xiaoying Y, Dongping L, Chen J, Ruimin S, Xueping L, Fangxing L. Synthesis and characterization of novel blood-compatible soluble chemically cross-linked polyurethanes with excellent mechanical performance for biomedical applications. *Biomacromolecules* 2005;6:1713–1721.
 16. Lligadas G, Ronda JC, Galia M, Cádiz, V. Polyurethane networks from fatty acid-based aromatic triols: Synthesis and characterization. *Biomacromolecules* 2007;8:1858–1864.
 17. Andjelkovic DD, Larock RC. Novel rubbers from cationic copolymerization of soybean oils and dicyclopentadiene 1. Synthesis and characterization. *Biomacromolecules* 2006;7:927–936.
 18. Guner FS, Yagci Y, Erciyes T. Polymers from triglyceride oils. *Prog Polym Sci* 2006;31:633–670.
 19. Kong X, Narine SS. Physical properties of polyurethane plastic sheets produced from polyols from canola oil. *Biomacromolecules* 2007;8:2203–2209.
 20. Lligadas G, Ronda JC, Galia M, Cádiz, V. Plant oils as platform chemicals for polyurethane synthesis: Current state-of-the-art. *Biomacromolecules* 2010;11:2825–2835.
 21. Gonzalez-Paz RJ, Lluch G, Lligadas G, Ronda JC, Galia M, Cádiz, V. A Green approach toward oleic and undecylenic acid-derived polyurethanes. *J Polym Sci Part A: Polym Chem* 2011;49:2407–2416.
 22. Thakore IM, Desai S, Sarawade BD, Devi S. Studies on biodegradability, morphology and thermomechanical properties of LDPE/modified starch blends. *Eur Polym J* 2001;7:151–160.
 23. Kim SU, Heo DN, Lee JB, Kim JR, Park SH, Jeon SH, Kwon IK. Electrospun gelatin/polyurethane blended nanofibers for wound healing. *Biomed Mater* 2009;4:044106.
 24. Chiellini E, Cinelli P, Fernandes EG, Kenawy ES, Lazzeri A. Gelatin-based blends and composites. Morphological and thermal mechanical characterization. *Biomacromolecules* 2006;2:806–811.
 25. Nirmala R, Nam K, Navamathavan R, Park S-J, Kim H. Hydroxyapatite mineralization on the calcium chloride blended polyurethane nanofiber via biomimetic method. *Nanoscale Res Lett* 2011;6:2–8.
 26. Detta N, Errico C, Dinucci D, Puppi D, Clarke DA, Reilly GC, Chiellini F. Novel electrospun polyurethane/gelatin composite meshes for vascular grafos. *J Mater Sci Mater Med* 2010;21:1761–1769.
 27. Cascone MG, Lazzeri L, Barbani N, Polacco G, Pollicino A, Giusti P. Dehydrothermally cross-linked collagen–poly(vinyl alcohol) blends: Mechanical, biological and surface properties. *J Mater Sci Mater Med* 1997;7:297–300.
 28. Ciardelli G, Chiono V. Materials for Peripherals nerve regeneration. *Macromol Biosci* 2006;6:13–26.
 29. Elbert DL, Hubbell JA. Surface treatments of polymers for compatibility. *Annu Rev Mater Sci* 1996;26:365–394.
 30. Horbett TA. The role of adsorbed proteins in animal cell adhesion. *Colloid Surf B Biointerfaces* 1994;2:225–240.
 31. Anselme K. Osteoblast adhesion on biomaterials. *Biomaterials* 2000;21:667–681.
 32. Hajiali H, Shahgasempour S, Naimi-Jamal MR, Peirovi H. Electrospun PGA/gelatin nanofibrous scaffolds and their potential application in vascular tissue engineering. *Int J Nanomed* 2011;6:2133–2141.
 33. Ebisawa Y, Kokubo T, Ohura K, Yamamuro T. Bioactivity of CaO-SiO₂-based glasses: In vitro evaluation. *J Mater Sci Mater Med* 1990;1:239–244.
 34. He Y, Zhu B, Inoue Y. Hydrogen bonds in polymers blends. *Prog Polym Sci* 2004;29:1021–1051.
 35. Chandrasekaran AR, Venugopla J, Sundarajan S, Ramakrishna S. Fabrication of nanofibrous scaffold with improved bioactivity for cultured of human dermal fibroblast for skin regeneration. *Biomed Mater* 2011;6:015001.
 36. Roccatone D, Fioroni M, Zacharias M, Colombo G. Effect of hexafluoroisopropanol alcohol on the structure of melittin: A molecular dynamics simulation study. *Protein Sci* 2005;14:2582–2589.
 37. Williams DF, editor. *Definitions in Biomaterials*. Amsterdam: Elsevier;1987.
 38. Schweizer S, Taubert A. Polymer-controlled, bio-inspired calcium phosphate mineralization from aqueous solution. *Macromol Biosci* 2007;7:1085–1099.
 39. Kumta PN, Sfeir C, Lee D, Olton D, Choi D. Nanostructured calcium phosphates for biomedical applications: Novel síntesis and characterization. *Acta Biomater* 2005;1:65–83.
 40. Dorozhkin SV, Epple M. Biological and medical significance of calcium phosphates. *Angew Chem Int Ed* 2002;41:3130–3146.
 41. Termine JD, Posner AS. Infrared determination of the percentage of crystallinity in apatitic calcium phosphate. *Nature* 1966;211:268–270.
 42. Owen GRh, Meredith DO, ap Gwynn I, Richards RG. Focal adhesion quantification—A new assay of material biocompatibility? Review. *Eur Cell Mater* 2005;9:85–96.
 43. Neff JA, Tresco PA, Caldwell KD. Surface modification for controlled studies of cell-ligand interactions. *Biomaterials* 1999;20:2281–2286.